found at 36.0 cM on chromosome 6 (LOD = 3.787) and at 64.0 cM on chromosome 7 (LOD = 5.314), and suggestive linkage was found on chromosomes 3, 5, 12 and 17 (Figure 3C). Taken together, Figure 3A–C shows that the same two markers, D7SNP32 at 53.6 cM and C7.loc64 at 64.0 cM on chromosome 7, defined the linkage peak in all three papilloma size categories (all sizes, <2 mm, 2–6 mm), suggesting that the same gene or set of genes may be involved.

Finally, linkage analysis was conducted on the basis of multiplicity of papillomas >6 mm in diameter. Significant linkage was found only at 44.7 cM on chromosome 4 (LOD = 5.358) in $p53^{+/+}$ mice (Supplementary Figure 1F, available at *Carcinogenesis* Online). In $p53^{+/-}$ mice, strong linkage was identified at 38.0 cM on chromosome 11 in a region that overlaps with *p53*, and suggestive linkage was found on chromosome 4 (Supplementary Figure 1G, available at *Carcinogenesis* Online). Combined results showed almost the same results as that of $p53^{+/+}$ mice, but the LOD score of the linkage locus on chromosome 4 increased to almost seven (LOD = 6.992; Figure 3D). The strong linkage to smaller size (<6 mm) of papillomas was found on chromosome 7; however, this region did not show any linkage to larger size (>6 mm) of papillomas. These results clearly suggest papillomas at early and later stages are under distinct genetic control.

To narrow down the identified linkage regions, precise genotyping was performed with additional 10 informative microsatellite markers on chromosomes 7 and 4. As a result, two peaks were observed on chromosome 7. Highly significant linkage for the papilloma multiplicity was mapped between D7SNP507 and D7SNP513 (interval was 25.2 Mb in size) and between D7SNP6 and D7Mit10 (interval was 10 Mb in size) (Figure 4A). A maximum LOD score of 6.974 was mapped at the D7SNP32 and 6.780 at the C7.loc64 individually. Significant linkage for the larger papilloma multiplicity was mapped between D4Mit174 and D4Mit15 (interval was 10.7 Mb in size) (Figure 4B). A maximum LOD score of 6.992 was mapped at the D4SNP14.

Genetic screening of carcinoma modifiers

In order to search for loci that might be associated with carcinoma development, linkage analysis on the basis of carcinoma development was carried out. Linkage analysis of $p53^{+/+}$ and $p53^{+/-}$ mice was done separately. As a result, strong linkage (LOD = 4.049) was detected at D4Mit43 at 60.4 cM on chromosome 4 in $p53^{+/+}$ F1 backcross mice (Figure 5A). The linkage peak at the D4SNP43 is close to the peak at the D4SNP14, which was linked to larger size of papillomas (Figures 3D and 4B). This is probably due to the same gene conferring resistance to larger size papillomas and carcinomas. Next, when we performed linkage analysis of $p53^{+/-}$ F1 backcross mice, surprisingly, the chromosome 4 linkage peak detected in the $p53^{+/+}$ group totally disappeared. Instead, linkage was found on chromosome 5 and

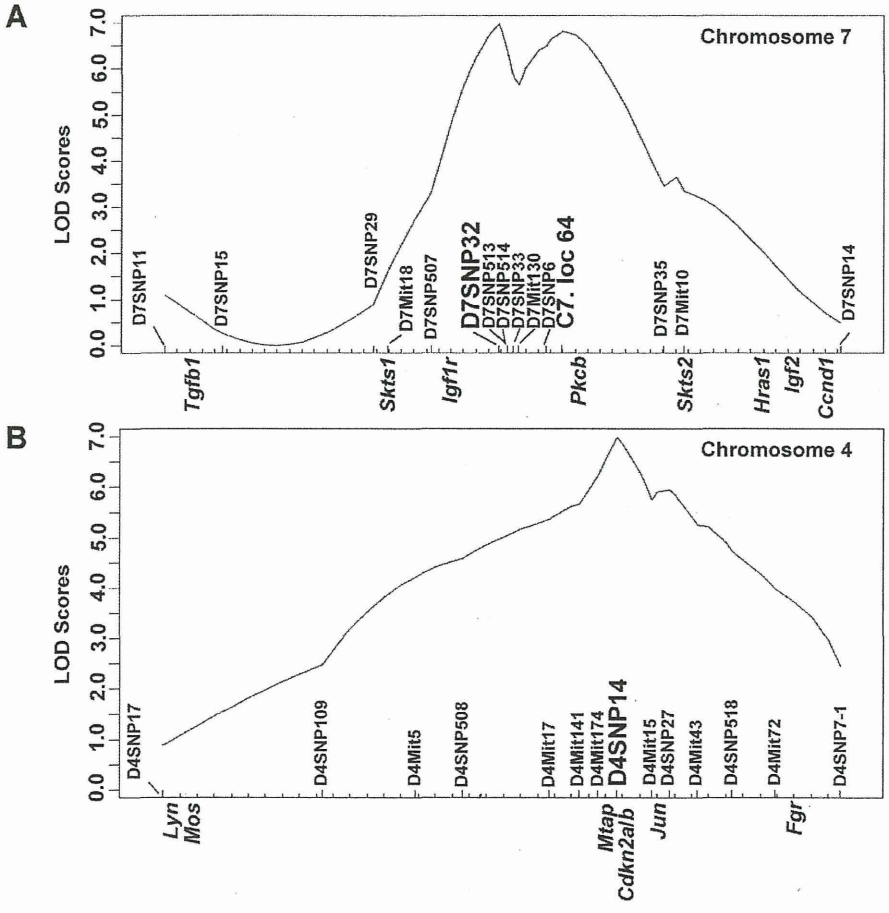

Fig. 4. Interval mapping for papilloma multiplicity QTL on chromosomes 4 and 7. By analyzing 228 ($p53^{+/+}$ and $p53^{+/-}$) FVB/N × (FVB/N × MSM/Ms) F1 backcross mice (**A**) two highly significant linkage were mapped at D7SNP32 (LOD: 6.974, position: 90 288 288 bp) and C7.loc64 (LOD: 6.811) on chromosome 7 for total papilloma number at 20 weeks after initiation. C7.loc64 is the peak position predicted by J/qtl. Several well-known genes located on chromosome 7 are indicated. (**B**) Highly significant linkage for number of larger papilloma (>6 mm) at 20 weeks after initiation was mapped at D4SNP14 (LOD: 6.992, position: 85 877 570 bp) on chromosome 4. Several well-known genes located on chromosome 4 are indicated.

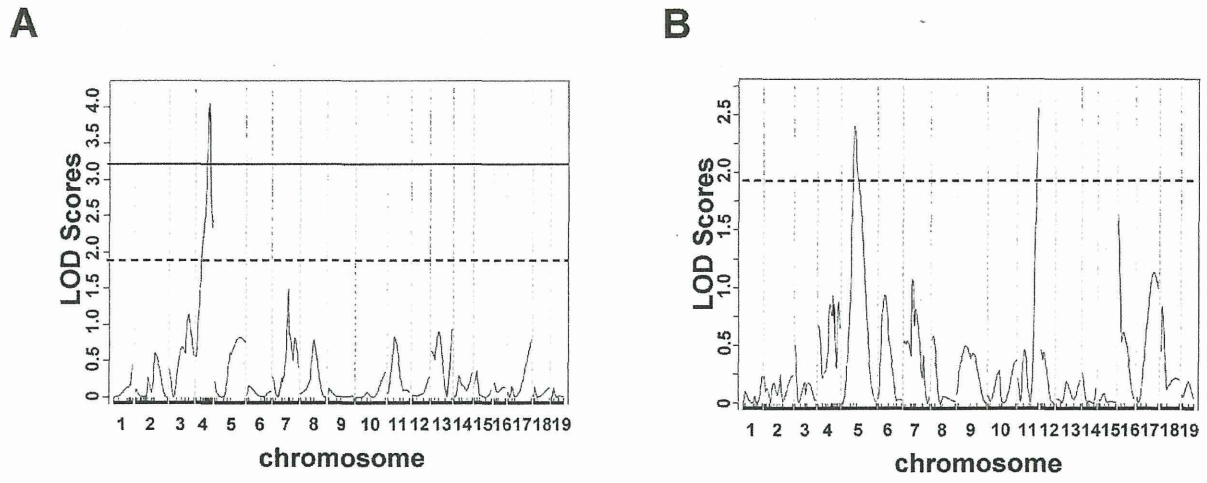

Fig. 5. Linkage analysis of QTL for carcinoma number in $p53^{+/-}$ FVB/N × (FVB/N × MSM/Ms) F1 backcross mice ($n = 107$) and $p53^{+/+}$ FVB/N × (FVB/N × MSM/Ms) F1 backcross mice ($n = 121$). (**A**) Whole-genome scanning of 121 $p53^{+/+}$ mice. Linkage analysis revealed a single highly significant linkage on chromosome 4 for carcinoma number at 40 weeks after initiation. (**B**) Whole-genome scanning of 107 $p53^{+/-}$ mice. Linkage analysis revealed suggestive linkage on chromosomes 5 and 11 for carcinoma number at 40 weeks after initiation. Dashed line indicates empirical suggestive and significant linkages of LOD score at 1.9 and 3.3.

distal chromosome 11, although these reached only a suggestive significance level (Figure 5B). The D11SNP8 on distal chromosome 11 showed linkage to papilloma multiplicity in $p53^{+/-}$ mice (Supplementary Figure 1B and E, available at *Carcinogenesis* Online) as well. When both genotypes were combined, suggestive linkage on chromosome 7, and in the middle of chromosome 11 were seen in addition to the significant linkage on chromosomes 4 and suggestive linkage on chromosome 5 (Supplementary Figure 1H, available at *Carcinogenesis* Online). The third column to the bottom of Table 1 suggests FVB/N/MSM/Ms heterozygous genotype at D5SNP12 in the carcinoma linkage region was associated with carcinoma prone phenotype. FVB/N/FVB/N homozygous genotype was associated with carcinoma-free phenotype. In other words, MSM/Ms allele at D5SNP12 conferred susceptibility to carcinoma development, whereas the FVB/N allele at the same locus conferred resistance.

Allele-specific mutation of Hras and allelic imbalance analysis of distal chromosome 7

The locations of *Skts 2* and *Hras* on distal chromosome 7 are in proximity to the linkage peak at C7.loc 64 in this study (Figure 4A). We, therefore, investigated the possibility that the linkage at C7.loc 64 influenced the allele-specificity of *Hras* gene alterations (31). Sequence analysis of *Hras* exon 2 identified a *BsmAI* restriction site polymorphism between FVB/N and MSM/Ms (Supplementary Figure 2A, available at *Carcinogenesis* Online). The somatic codon 61 mutation introduces a restriction site for the enzyme *XbaI*, as reported previously (31). If the mutation occurs on MSM/Ms allele, this can be detected by the presence of a 91 bp band after double digestion with *BsmAI* and *XbaI* (Supplementary Figure 2A, available at *Carcinogenesis* Online). The majority of papillomas (36/40) produced 91 and 116 bp bands by a single digestion with *XbaI* (data not shown), indicating the presence of the *Hras* codon 61 mutation. In the *XbaI* and *BsmAI* double digestion, the 91 bp band was retained in 12 papillomas (Supplementary Figure 2B, available at *Carcinogenesis* Online), indicating that these papillomas had the *Hras* mutation on the MSM/Ms allele. In the remaining 28 papillomas, the mutation must have occurred on the FVB/N allele, and this difference is statistically significant ($P < 0.01$, by Fisher test). We next performed allelic imbalance analysis using microsatellite markers on distal chromosome 7 (Supplementary Figure 2C, available at *Carcinogenesis* Online). Preferential allelic imbalance in favor of the FVB/N allele in the chromosomal region that included *Hras* was observed in 20 of 30 papillomas (Supplementary Figure 2D, available at *Carcinogenesis* Online). In only one case did the imbalance involved the MSM/Ms allele ($P < 0.01$ by Fisher test). These results are consistent with a previous study reporting that *Skts2* has an influence on the allelic preference *of Hras* gene alteration (31).

Discussion

This study shows that MSM/Ms is a dominant resistant strain in the two-stage skin carcinogenesis, when crossed with highly susceptible FVB/N mice. Among the 10 mice in each group, no MSM/Ms developed papillomas, and only a few F1 (FVB/MSM/Ms) hybrid mice developed one or two papillomas. In a population of 228 F1 backcross mice, highly significant QTLs for papilloma development with a maximum LOD score of 7.0 were mapped to chromosomes 7 and 4. A suggestive QTL for carcinoma development was mapped to chromosome 5.

We classified papillomas into three categories based on their diameter, and carried out linkage analysis for each category. Linkage analysis revealed strong linkage at D7SNP32 and C7.loc64 on chromosome 7 to total papilloma number, number of papillomas <2 mm and number of papillomas of 2–6 mm in size. However, these linkage peaks at D7SNP32 and C7.loc64 completely disappeared when the analysis was confined to papillomas >6 mm. These results indicate that a corresponding gene on chromosome 7 functions only at an early papilloma stage, but is not involved at the later stage of papilloma progression, although it is not clear at this stage whether it is involved in initiation. The physical positions of these linkage peaks at D7SNP32 and C7.loc64 are close to *Skts1* and *Skts2* (9), two of the skin tumor susceptibility loci previously mapped to 30–35 cM and 70–80 cM on chromosome 7, respectively, in a NIH and *Mus spretus* interspecific backcross. The location of *Skts1* was refined by using a large series of congenic lines (32), moving it more proximally than originally reported (9). The distance was narrowed to the 4–5 cM region (in the present MGI database, http://www.informatics.jax.org), which is located between D7SNP29 and D7SNP507 in Figure 4A. Two linkage peaks were detected at D7SNP32 and C7.loc64 in our study (Figure 4A) that may correspond to *Skts1* and *Skts2*, respectively. The use of congenic lines will enable further refinement of *Skts1* or *2*, and possibly leading to the identification of the involved genes. The proximal interval including *Skts1* region still contains a large number of genes, some of which (e.g. *R-ras*, *Tsg101*, *Necdin*, *Atp10a* and

Table 1. Markers showing the highest LOD score in each tumor category F × FM: FVB × (FVB × MSM/Ms), FF: FVB/FVB allele, FM: FVB/MSM/Ms allele C7.loc64, c11.loc38 and c5.loc52 are peak position predicted by J/qtl. Closest genotyped markers (D7SNP6, D11SNP11 and D5SNP12) are shown in parallel.

F × FM backcross mice	Tumor category	Chromosome no.	Marker	rs no.	Map position (cM)	Map position (bp)	Tumor number	FF (%)	FM (%)	LOD score
$p53^{+/+}$ and $p53^{+/-}$ combined ($n = 228$)	Papilloma size is <2 mm at 20 weeks	7	D7SNP32	rs32219681	53.6	90288288	0 ($n = 109$)	34.9	65.1	4.869
							>0 ($n = 119$)	64.4	35.6	
	Papilloma size is 2–6 mm at 20 weeks	7	D7SNP6	rs3023159	—	126426677	0 ($n = 57$)	23.2	76.8	5.005
							>0 ($n = 171$)	56.1	43.9	
			c7.loc64	—	64.0	—	—	—	—	5.314
							—	—	—	
	Papilloma size is >6 mm at 20 weeks	4	D4SNP14	rs3710891	53.3	85877570	0 ($n = 141$)	32.6	67.4	6.992
							>0 ($n = 87$)	81.1	18.9	
	Total papilloma at 20 weeks	7	D7SNP32	rs32219681	53.6	90288288	0 ($n = 40$)	20.0	80.0	6.974
							>0 ($n = 188$)	56.7	43.3	
	Total carcinoma at 40 weeks	4	D4SNP27	rs4137854	59.5	98819537	0 ($n = 109$)	38.5	61.5	4.410
							>0 ($n = 119$)	66.4	33.6	
$p53^{+/+}$ ($n = 121$)	Papilloma size is <2 mm at 20 weeks	7	D7SNP513	rs31348773	55.0	98225267	0 ($n = 51$)	21.6	78.4	5.063
							>0 ($n = 70$)	58.6	41.4	
	Papilloma size is 2–6 mm at 20 weeks	7	D7SNP32	rs32219681	53.6	90288288	0 ($n = 33$)	24.2	75.8	3.921
							>0 ($n = 88$)	52.9	47.1	
	Papilloma size is >6 mm at 20 weeks	4	D4SNP14	rs3710891	53.3	85877570	0 ($n = 71$)	27.5	72.5	5.358
							>0 ($n = 50$)	76.0	24.0	
	Total papilloma at 20 weeks	7	D7SNP32	rs32219681	53.6	90288288	0 ($n = 25$)	24.0	76.0	5.109
							>0 ($n = 96$)	50.5	49.5	
	Total carcinoma at 40 weeks	4	D4Mit43	—	60.3	107406076	0 ($n = 68$)	30.9	69.1	4.049
							>0 ($n = 53$)	69.9	30.1	
$p53^{+/-}$ ($n = 107$)	Papilloma size is <2 mm at 20 weeks	None	—	—	—	—	—	—	—	—
							—	—	—	
	Papilloma size is 2–6 mm at 20 weeks	11	D11SNP8	rs3023316	86.4	117028591	0 ($n = 24$)	17.3	82.6	3.036
							>0 ($n = 83$)	42.7	57.3	
	Papilloma size is >6 mm at 20 weeks	11	D11SNP11	rs3714172	—	75418964	0 ($n = 70$)	8.6	91.4	0.433
							>0 ($n = 37$)	8.1	91.9	
			c11.loc38	—	38.0	—	—	—	—	14.853
							—	—	—	
	Total papilloma at 20 weeks	11	D11SNP8	rs3023316	86.4	117028591	0 ($n = 14$)	7.1	92.9	3.555
							>0 ($n = 93$)	41.8	58.2	
	Total carcinoma at 40 weeks	5	D5SNP12	rs13478361	—	83810839	0 ($n = 41$)	65.9	34.1	2.383
							>0 ($n = 66$)	31.8	68.2	
			c5.loc52	—	52.0	—	—	—	—	2.405
							—	—	—	
		11	D11SNP8	rs3023316	86.4	117028591	0 ($n = 41$)	12.2	87.8	2.559

Ube3a) are interesting candidate genes for future study. Several important candidate genes are located in the distal interval on chromosome 7, including *Pkcb*, *Hras*, etc. *Ras* genes have been implicated in cancer predisposition in both human and mouse. The initiating event for mouse skin tumors induced by treatment with DMBA involves mutation of the *Hras* gene at codon 61 (33). This mutation is detected in 90% of papillomas and carcinomas and is followed by trisomy of chromosome 7, on which *Hras* is located, leading to preferential duplication of the mutant allele (34). A previous study also demonstrated the influence of *Skts2* on allele-specific mutations in *Hras* gene (31). The mouse *Hras* gene had specific activating mutations in the *Mus musculus* allele in 90% of DMBA-TPA-induced carcinomas in NIH/*Mus spretus* crosses. In all cases, tumors with *Hras* mutations also showed specific imbalance of chromosome 7 markers that favored the chromosome carrying the mutant allele. Frequent mutations were detected on FVB/N allele of the *Hras* gene, and high frequency of allelic imbalance in favor of FVB/N allele of the *Hras* gene was also found in our study, as well as in *Mus spretus* study. These results suggest the linkage peak at C7.loc64 on chromosome 7 showed the same effect on the allele -specificity of *Hras* mutation as *Skts2*, suggesting that a common gene might be responsible for *Skts2* and the linkage at C7.loc64. In this interval, some other QTLs for susceptibility to other types of tumors have been mapped, including the lung cancer susceptibility loci *Sluc8* and *Sluc19* (4). *Tlsm1* has been mapped as locus conferring susceptibility to lymphoma (35).

Highly significant linkage to larger papilloma size (>6 mm) was found at D4SNP14 on chromosome 4. This locus did not have any effect on smaller papilloma size or on total number of all size of papillomas. Interestingly, 81.1% of the F1 backcross mice that developed papillomas >6 mm in size were FVB/N allele homozygous at D4SNP14 (Table 1). When compared with other loci in Table 1, this ratio of FVB/N homozygous genotype in tumor prone animals is higher, suggesting that FVB/N allele at this locus confers strong susceptibility to increased papilloma growth. On the other hand, 80.0% of papilloma-free mice are FVB/N/MSM/Ms heterozygous at D7SNP32 (fifth column from the top of Table 1), suggesting that the MSM/Ms allele at this locus confers strong resistance.

Significant linkage to carcinoma development was found on chromosome 4 in the region associated with late-stage papilloma development. This finding could give us a clue to obtain an answer for a very fundamental question. Skin tumor progression takes place in a number of steps, starting with *ras* mutation, passing through benign papillomas, some of them progress to carcinoma. However, it is not known whether passage through papilloma to carcinoma is linear, or involves different independent pathways. If the pathway was linear, it would be expected that a locus that confers resistance to papillomas would similarly prevent progression to carcinomas. A strong resistant carcinoma locus on chromosome 4, detected in this study, significantly affects late-stage papillomas, but it does not have any effect on early stage papillomas. These results suggest that a corresponding gene on this locus plays a role in the growth of later stage papilloma instead of papillomagenesis and directly regulates the transition from papilloma to carcinoma. However, the loci detected

in this study seem to exert their effects mainly at different stage of tumorigenesis. MSM/Ms allele at the significant resistant papilloma locus on chromosome 7 seems to confer resistance only to papilloma development, but have no effect on carcinoma development. On the other hand, a suggestive carcinoma locus mapped on chromosome 5 has no effect on papilloma development. It seems probably that a very limited number of linear pathway regulating the progression through papilloma to carcinoma are genetically modified by other different independent pathways.

Skts7 and *Skts-fp1* were mapped at 40–60 cM on chromosome 4 for chemically induced skin papilloma susceptibility by the analysis of NIH and *Mus spretus* cross, and FVB and PWK cross, respectively (17,18). A common gene might be responsible for the susceptibility of these two and our crosses. PWK, *Mus spretus* and MSM/Ms are wild-derived inbred strains that could share common haplotypes. The haplotype analysis would help to identify a candidate gene in the near future. This region contains many QTLs for susceptibility to other types of tumors (6). *Pctr1* and *Pctr2* were mapped as loci for susceptibility to pristane-induced plasmacytoma (36,37), and *Cdkn2a* has been suggested to be a corresponding gene for *Pctr1* (38,39). *Cdkn2a* is also a strong candidate gene for *Papg1*, QTL for progression of urethane-induced lung tumors (40). This could be a good candidate gene for late-stage papilloma and carcinoma on chromosome 4 in our study. The *Cdkn2a* locus encodes two separate proteins (*Cdkn2a*, also known as p16, and $p19^{Arf}$) generated from alternative open reading frames. The $p19^{Arf}$ protein activates p53 signaling through an interaction with Mdm2 (41). A previous study demonstrated that more papillomas were induced in $p19^{Arf}$-deficient mice, compared with wild-type mice using the DMBA/TPA two-step protocol. Relative to wild-type mice, the size of papillomas was larger in $p19^{Arf}$-deficient mice. Malignant conversion of papillomas to squamous cell carcinomas was markedly accelerated in $p19^{Arf}$-deficient mice (42). Our data showing the complete disappearance of the chromosome 4 modifier locus in $p53^{+/-}$ mice suggest that $p19^{Arf}$ may play a major role in the transition to large papillomas and carcinomas. It might be expected that reduced gene dosage of *p53* reduces the effect of any polymorphism that affects the levels or function of $p19^{Arf}$ in controlling p53 activity. In this case, the linkage becomes entirely dependent on whether the backcross animal carries the *p53* null allele, which would explain the very strong linkage of papilloma size to the *p53* locus in the $p53^{+/-}$ backcross population.

Linkage positively regulated in a *p53*-dependent manner was seen also on chromosomes 3, 11 and 13 as well as on chromosome 4 for total and intermediate size papilloma number. Whereas negatively regulated linkage was seen on chromosomes 12 and 17 (Supplementary Figure 1A, 1B, 1D, E and Supplementary Table 2, available at *Carcinogenesis* Online). Another carcinoma locus that is negatively regulated in a *p53*-dependent manner, conferring susceptibility was found on chromosome 5 in this study. The main reason why we used *p53* knockout F1 backcross mice was to increase carcinoma incidence and map significant *p53*-dependent carcinoma modifiers. But the number of $p53^{+/-}$ F1 backcross mice treated with DMBA/TPA was relatively small (n = 107), clear linkage positively or negatively regulated in a *p53*-dependent manner for carcinoma was seen only on chromosomes 4 and 5. Although the linkage on chromosome 5 reached only a suggestive significance level and the region was still quite big, DMBA/TPA treatment using more mice would simply strengthen the linkage and facilitate gene identification in this region.

MSM/Ms is a wild-derived inbred strain that has high genetic diversity in comparison with standard inbred strains (26). We expected to have a large genetic variation to skin tumor susceptibility between FVB/N and MSM/Ms. We successfully mapped three significant loci on chromosomes 4, 6 and 7 and several suggestive loci. Many tumor susceptibility loci were mapped on the same chromosomal regions where skin tumor susceptibility loci were mapped in this study. Conventional methods, such as haplotype analysis, congenic and recombinant inbred strains, together with bioinformatic analysis based on the accumulated SNP data will facilitate the following gene identification step.

Supplementary material

Supplementary Table 1 and 2 and Figures 1 and 2 can be found at http://carcin.oxfordjournals.org/

Funding

MEXT's program "Promotion of Environmental Improvement for Independence of Young Researchers" under the Special Coordination Funds for Promoting Science and Technology at Niigata University.

Acknowledgements

We thank Drs Minh To and Allan Balmain for critical reading of this article.

Conflict of Interest Statement: None declared.

References

1. Balmain,A. (2002) Cancer as a complex genetic trait: tumor susceptibility in humans and mouse models. *Cell*, **108**, 145–152.
2. Balmain,A. *et al.* (2003) The genetics and genomics of cancer. *Nat. Genet.*, **33 Suppl**, 238–244.
3. Dietrich,W.F. *et al.* (1993) Genetic identification of Mom-1, a major modifier locus affecting Min-induced intestinal neoplasia in the mouse. *Cell*, **75**, 631–639.
4. Fijneman,R.J. *et al.* (1996) Complex interactions of new quantitative trait loci, Sluc1, Sluc2, Sluc3, and Sluc4, that influence the susceptibility to lung cancer in the mouse. *Nat. Genet.*, **14**, 465–467.
5. Ruivenkamp,C.A.L. *et al.* (2002) Ptprj is a candidate for the mouse colon-cancer susceptibility locus Scc1 and is frequently deleted in human cancers. *Nat. genet.*, **31**, 295–300.
6. Demant,P. (2003) Cancer susceptibility in the mouse: genetics, biology and implications for human cancer. *Nat. Rev. Genet.*, **4**, 721–734.
7. Dragani,T.A. (2003) 10 years of mouse cancer modifier loci: human relevance. *Cancer Res.*, **63**, 3011–3018.
8. Mao,J.H. *et al.* (2003) Genomic approaches to identification of tumour-susceptibility genes using mouse models. *Curr. Opin. Genet. Dev.*, **13**, 14–19.
9. Nagase,H. *et al.* (1995) Distinct genetic loci control development of benign and malignant skin tumours in mice. *Nat. Genet.*, **10**, 424–429.
10. To,M.D. *et al.* (2006) A functional switch from lung cancer resistance to susceptibility at the Pas1 locus in Kras2LA2 mice. *Nat. Genet.*, **38**, 926–930.
11. Santos,J. *et al.* (2002) A new locus for resistance to gamma-radiation-induced thymic lymphoma identified using inter-specific consomic and inter-specific recombinant congenic strains of mice. *Oncogene*, **21**, 6680–6683.
12. Ewart-Toland,A. *et al.* (2003) Identification of Stk6/STK15 as a candidate low-penetrance tumor-susceptibility gene in mouse and human. *Nat. Genet.*, **34**, 403–412.
13. Peissel,B. *et al.* (2000) Linkage disequilibrium and haplotype mapping of a skin cancer susceptibility locus in outbred mice. *Mamm. Genome*, **11**, 979–981.
14. Wakabayashi,Y. *et al.* (2007) Promotion of Hras-induced squamous carcinomas by a polymorphic variant of the *Patched* gene in FVB mice. *Nature*, **445**, 761–765.
15. Angel,J.M. *et al.* (1997) Association of a murine chromosome 9 locus (Psl1) with susceptibility to mouse skin tumor promotion by 12-O-tetradecanoylphorbol-13-acetate. *Mol. Carcinog.*, **20**, 162–167.
16. Angel,J.M. *et al.* (2003) Identification of novel genetic loci contributing to 12-O-tetradecanoylphorbol-13-acetate skin tumor promotion susceptibility in DBA/2 and C57BL/6 mice. *Cancer Res.*, **63**, 2747–2751.
17. Fujiwara,K. *et al.* (2007) New chemically induced skin tumour susceptibility loci identified in a mouse backcross between FVB and dominant resistant PWK. *BMC Genet.*, **8**, 39.
18. Fujiwara,K. *et al.* (2010) New outbred colony derived from *Mus musculus castaneus* to identify skin tumor susceptibility loci. *Mol. Carcinog.*, **49**, 653–661.
19. Moriwaki,K. *et al.* (2009) Unique inbred strain MSM/Ms established from the Japanese wild mouse. *Exp. Anim.*, **58**, 123–134.
20. Miyashita,N. *et al.* (1987) H-2-controlled genetic susceptibility to pulmonary adenomas induced by urethane and 4-nitroquinoline 1-oxide in A/Wy congenic strains. *Jpn. J. Cancer Res.*, **78**, 494–498.

21. Pataer,A. *et al.* (1996) Two dominant host resistance genes to pre-B lymphoma in wild-derived inbred mouse strain MSM/Ms. *Cancer Res.*, **56**, 3716–3720.
22. Okumoto,M. *et al.* (1995) Radiation-induced lymphomas in MSM (BALB/cHeA x MSM) F1 and (BALB/cHeA x STS/A) F1 hybrid mice. *Exp. Anim.*, **44**, 43–48.
23. Matsumoto,Y. *et al.* (1998) Allelic loss analysis of gamma-ray-induced mouse thymic lymphomas: two candidate tumor suppressor gene loci on chromosomes 12 and 16. *Oncogene*, **16**, 2747–2754.
24. Okamoto,M. *et al.* (2005) Intestinal tumorigenesis in Min mice is enhanced by X-irradiation in an age-dependent manner. *J. Radiat. Res.*, **46**, 83–91.
25. Kikkawa,Y. *et al.* (2001) Microsatellite database for MSM/Ms and JF1/Ms, molossinus-derived inbred strains. *Mamm. Genome*, **12**, 750–752.
26. Abe,K. *et al.* (2004) Contribution of Asian mouse subspecies *Mus musculus molossinus* to genomic constitution of strain C57BL/6J, as defined by BAC-end sequence-SNP analysis. *Genome Res.*, **14**, 2439–2447.
27. Abel,E.L. *et al.* (2009) Multi-stage chemical carcinogenesis in mouse skin: fundamentals and applications. *Nat. Protoc.*, **4**, 1350–1362.
28. Kemp,C.J. *et al.* (1993) Reduction of p53 gene dosage does not increase initiation or promotion but enhances malignant progression of chemically induced skin tumors. *Cell*, **74**, 813–822.
29. Masuya,H. *et al.* (2005) Enamelin (Enam) is essential for amelogenesis: ENU-induced mouse mutants as models for different clinical subtypes of human amelogenesis imperfecta (AI). *Hum. Mol. Genet.*, **14**, 575–583.
30. Broman,K.W. *et al.* (2003) R/qtl: QTL mapping in experimental crosses. *Bioinformatics*, **19**, 889–890.
31. Nagase,H. *et al.* (2003) Allele-specific Hras mutations and genetic alterations at tumor susceptibility loci in skin carcinomas from interspecific hybrid mice. *Cancer Res.*, **63**, 4849–4853.
32. de Koning,J.P. *et al.* (2007) Convergence of congenic mapping and allele-specific alterations in tumors for the resolution of the Skts1 skin tumor susceptibility locus. *Oncogene*, **26**, 4171–4178.
33. Quintanilla,M. *et al.* (1986) Carcinogen-specific mutation and amplification of Ha-ras during mouse skin carcinogenesis. *Nature*, **322**, 78–80.
34. Kemp,C.J. *et al.* (1993) Allelotype analysis of mouse skin tumors using polymorphic microsatellites: sequential genetic alterations on chromosomes 6, 7, and 11. *Cancer Res.*, **53**, 6022–6027.
35. Yamada,Y. *et al.* (1994) T lymphomagenesis is determined by a dominant host gene thymic lymphoma susceptible mouse-1 (TLSM-1) in mouse models. *J. Exp. Med.*, **180**, 2155–2162.
36. Potter,M. *et al.* (1994) Identification of two genes on chromosome 4 that determine resistance to plasmacytoma induction in mice. *Cancer Res.*, **54**, 969–975.
37. Mock,B.A. *et al.* (1997) The plasmacytoma resistance gene, Pctr2, delays the onset of tumorigenesis and resides in the telomeric region of chromosome 4. *Blood*, **90**, 4092–4098.
38. Zhang,S. *et al.* (1998) Cdkn2a, the cyclin-dependent kinase inhibitor encoding p16INK4a and p19ARF, is a candidate for the plasmacytoma susceptibility locus, Pctr1. *Proc. Natl. Acad. Sci. U.S.A.*, **95**, 2429–2434.
39. Zhang,S. *et al.* (2003) p16 INK4a gene promoter variation and differential binding of a repressor, the ras-responsive zinc-finger transcription factor, RREB. *Oncogene*, **22**, 2285–2295.
40. Zhang,Z. *et al.* (2002) A strong candidate gene for the Papg1 locus on mouse chromosome 4 affecting lung tumor progression. *Oncogene*, **21**, 5960–5966.
41. Kamijo,T. *et al.* (1998) Functional and physical interactions of the ARF tumor suppressor with p53 and Mdm2. *Proc. Natl. Acad. Sci. U.S.A.*, **95**, 8292–8297.
42. Kelly-Spratt,K.S. *et al.* (2004) p19Arf suppresses growth, progression, and metastasis of Hras-driven carcinomas through p53-dependent and-independent pathways. *PLoS Biol.*, **2**, E242.

Received February 28, 2012; revised July 18, 2012; accepted July 23, 2012

The EMBO Journal (2013) 32, 1183–1194
www.embojournal.org

SOURCE DATA TRANSPARENT PROCESS THE EMBO JOURNAL

Epigenetic *Thpok* silencing limits the time window to choose CD4$^+$ helper-lineage fate in the thymus

Hirokazu Tanaka[1,3], Taku Naito[1,3,4], Sawako Muroi[1], Wooseok Seo[1], Risa Chihara[1], Chizuko Miyamoto[1], Ryo Kominami[2] and Ichiro Taniuchi[1,*]

[1]Laboratory for Transcriptional Regulation, RIKEN Research Center for Allergy and Immunology, Yokohama, Japan and [2]Department of Molecular Genetics, Graduate School of Medical and Dental Sciences, Niigata University, Niigata, Japan

CD4$^+$ helper and CD8$^+$ cytotoxic T cells differentiate from common precursors in the thymus after T-cell receptor (TCR)-mediated selection. Commitment to the helper lineage depends on persistent TCR signals and expression of the ThPOK transcription factor, whereas a *ThPOK* cis-regulatory element, *ThPOK* silencer, represses *Thpok* gene expression during commitment to the cytotoxic lineage. Here, we show that silencer-mediated alterations of chromatin structures in cytotoxic-lineage thymocytes establish a repressive state that is epigenetically inherited in peripheral CD8$^+$ T cells even after removal of the silencer. When silencer activity is enhanced in helper-lineage cells, by increasing its copy number, a similar heritable *Thpok* silencing occurs. Epigenetic locking of the *Thpok* locus may therefore be an independent event from commitment to the cytotoxic lineage. These findings imply that long-lasting TCR signals are needed to establish stable *Thpok* expression activity to commit to helper T-cell fate and that full commitment to the helper lineage requires persistent reversal of silencer activity during a particular time window.

The EMBO Journal (2013) **32**, 1183–1194. doi:10.1038/emboj.2013.47; Published online 12 March 2013
Subject Categories: chromatin & transcription; immunology
Keywords: cell fate; epigenetics; gene silencing; T-cell development; ThPOK

Introduction

Differentiation of multi-potent precursors into a particular lineage upon exposure to stimuli from external environmental cues is accompanied by the expression of lineage-specific genes together with repression of alternative lineages, a process termed as lineage specification. As a consequence of sequential exposures to differentiation signals, specific gene expression signatures that confer unique cellular functions to differentiated cells are established (lineage commitment) (Cantor and Orkin, 2001; Murphy and Reiner, 2002; Rothenberg and Dionne, 2002). Mechanisms that guarantee the stable inheritance of established gene signatures even after multiple cell divisions enable differentiated cells to preserve their cell identity. Studies in the last decade have highlighted the crucial contributions of epigenetics in maintenance of gene expression status (Jenuwein and Allis, 2001; Probst *et al*, 2009; Bonasio *et al*, 2010). For instance, heterochromatin has been shown to be involved in heritable and stable gene repression (Henikoff, 2000), referred to as gene silencing, in part via relocating gene loci into specialized nuclear compartments such as the peri-nuclear lamina (Schneider and Grosschedl, 2007; Reddy *et al*, 2008). It is thus conceivable that lineage commitment would involve epigenetic changes towards heterochromatin-like structures at many developmentally regulated genes to assure their subsequent silent state. However, how the epigenetic machinery that delivers lineage-specific epigenetic marks is linked with lineage commitment remains uncharacterized. Specifically, it is not clear whether such epigenetic machinery becomes functional upon lineage commitment or acts in parallel with lineage specification. In order to better understand an epigenetic link between environmental cues and establishment of cell identity, it is important to unravel how specific epigenetic modifications are accumulated on the relevant genes.

There are two major lineages of T lymphocytes, the CD4$^+$ helper and the CD8$^+$ cytotoxic cells, and they differentiate from a common precursor, the CD4$^+$CD8$^+$ double-positive (DP) thymocyte, after positive selection. During this selection process, only DP thymocytes that receive optimal TCR-signal strength as a result of TCR engagement with peptide–MHC complexes are allowed to further differentiate (Germain, 2002; Starr *et al*, 2003; Singer *et al*, 2008). When CD4$^+$CD8$^+$ DP thymocytes are positively selected through MHC class II molecules (MHC class II-selected thymocytes), they develop into CD4$^+$CD8$^-$ single-positive (SP) thymocytes that are committed to the helper lineage. On the contrary, DP thymocytes that undergo selection via MHC class I molecules with a help of CD8 co-receptors terminate CD4 expression and differentiate into CD4$^-$CD8$^+$ SP thymocytes committed to the cytotoxic lineage (Ellmeier *et al*, 1999). It has been proposed that differences in TCR-signal length during positive selection instruct distinct fates in post-selection thymocytes. Several lines of evidence have shown that persistent TCR signalling is essential for development of CD4$^+$ helper T cells (Sarafova *et al*, 2005; Singer *et al*, 2008; Adoro *et al*, 2012). On the other hand, temporary termination of *Cd8* gene expression in post-selection thymocytes (Brugnera *et al*, 2000) results in a disruption of TCR signals specifically in MHC class I-selected thymocytes, instructing them to become cytotoxic-lineage cells (Singer *et al*, 2008). However, it remains obscure why long-lasting TCR signals are necessary for commitment to the helper lineage.

*Corresponding author. Laboratory for Transcriptional Regulation, RIKEN Research Center for Allergy and Immunology, 1-7-22 Suehiro-cho, Tsurumi-ku, Yokohama, Kanagawa 230-0045, Japan.
Tel.: +81 45 503 7044; Fax: +81 45 503 7043;
E-mail: taniuchi@rcai.riken.jp
[3]These authors contributed equally to this work.
[4]Present address: Department of Molecular Immunology, Toho University School of Medicine, Tokyo, Japan.

Received: 19 October 2012; accepted: 6 February 2013; published online: 12 March 2013

Recently, it has been recognized that appropriate linkage of TCR specificity to MHC class during helper/cytotoxic lineage choice requires input from the zing finger transcription factor ThPOK (also known as cKrox), which is encoded by the *Zbtb7b* gene (hereafter referred to as the *Thpok* gene in this manuscript) (He *et al*, 2005, 2010; Sun *et al*, 2005). Gain and loss of function studies of ThPOK demonstrated a dominant role of ThPOK in acquiring a $CD4^+CD8^-$ phenotype that is independent of TCR specificity to MHC class. Thus, both MHC class I-selected and class II-selected thymocytes are redirected to alternative $CD4^+CD8^-$ helper and $CD4^-CD8^+$ cytotoxic lineages by ectopic induction or loss of ThPOK function, respectively (He *et al*, 2005; Sun *et al*, 2005). Because of its potent activity, expression of the *Thpok* gene from its two promoters, distal P1 and proximal P2, must be strictly regulated during thymocyte differentiation. During thymocyte maturation, ThPOK first appears after positive selection, increases in MHC class II-selected thymocytes, but then disappears in MHC class I-selected cells (He *et al*, 2005; Muroi *et al*, 2008). In sorting out mechanisms that control lineage- and stage-specific *Thpok* expression, previous studies have identified two essential *cis*-regulatory elements. A transcriptional silencer (referred to as the *Thpok* silencer in this manuscript) is essential to control helper lineage-specific expression of *Thpok* (He *et al*, 2008; Setoguchi *et al*, 2008). On the other hand, a transcriptional enhancer in the proximal region of the gene plays an essential role in increasing *Thpok* expression at later maturation stages in MHC class II-selected thymocytes (Muroi *et al*, 2008). Interestingly, conditional ablation of ThPOK function from peripheral $CD4^+$ T cells indicated that extra-thymic expression of ThPOK is still necessary to maintain $CD4^+$ helper T-cell identity (Wang *et al*, 2008). Furthermore, retroviral transduction of ThPOK into fully differentiated peripheral $CD8^+$ T cells can activate helper lineage-related genes as well as repress cytotoxic-related genes, albeit only to limited extent (Jenkinson *et al*, 2007). These findings indicate that the helper lineage-specific *Thpok* expression established in the thymus must be sustained in the peripheral T cells to maintain their lineage identity. However, although roles of *cis*-regulatory elements in regulating *Thpok* expression during lineage commitment in thymus have begun to be characterized (Taniuchi, 2009), it remains unknown how the established state of the *Thpok* gene, either active or repressive, is stably maintained in differentiated T cells.

To address this point, we used genetic approaches that enabled us to modify *Thpok* silencer activity. We show that a silencer-dependent deposition of repressive epigenetic marks establishes a repressive state that is inherited independently of the silencer in peripheral $CD8^+$ T cells via inhibiting the two promoters by different mechanisms. Furthermore, we provide evidence showing that such epigenetic *Thpok* silencing can also occur in $CD4^+$ helper-lineage cells when silencer activity persists after positive selection. These findings suggest that epigenetic mechanisms that lock the *Thpok* locus can take place even in MHC class II signalled cells if the silencer activity is not properly terminated. Thus, our findings strongly suggest that, for appropriate helper-lineage choice by MHC class II-selected cells, reversal of the *Thpok* silencer upon receipt of TCR signals must persist for a certain time interval to avoid epigenetic sealing of the *Thpok* gene. We thus propose that such continuous counter-silencing by long-lasting TCR signals is necessary to establish stable *Thpok* expression, hence to fully commit to helper T-cell fate.

Results

Epigenetic modifications in the Thpok gene

There is now compelling evidence that developmentally regulated genes receive dynamic modifications of local chromatin structure (Bonasio *et al*, 2010), and in particular, heterochromatin-like structures are known to be involved in stable gene repression (Henikoff, 2000). We therefore examined how the chromatin structure at the *Thpok* locus is altered during T-cell development. Since tri-methylation at two distinct histone H3 lysine residues, lysine 4 and lysine 27 (H3K4me3 and H3K27me3), has been shown to mark active and repressive states, respectively (Bernstein *et al*, 2005), of the target genes, we performed chromatin immunoprecipitation (ChIP)-on-chip analysis of distinct T-cell subsets. Accumulation of the repressive H3K27me3 mark at the distal P1 promoter and its upstream region was detected from immature $CD4^-CD8^-$ DN thymocytes onward in cell subsets that do not express *Thpok*, while it was not present at a significant level at the proximal P2 promoter (Figure 1A and C). In contrast, H3K27me3 deposition at the distal P1 promoter was replaced by active H3K4me3 marks in cells expressing *Thpok*, such as $CD4^+CD8^-$ SP thymocytes, along with accumulation of H3K4me3 at the proximal P2 promoter (Figure 1A). Interestingly, a comparison of the *Thpok* silencer-deficient and wild-type *Thpok* loci by analytical ChIP assays revealed that the loss of the *Thpok* silencer resulted in not only a decrease in H3K27me3 marks but also an increase in H3K4me3 marks around the P1 promoter in DP thymocytes (Figure 1B and C). Similar changes resulting from loss of the silencer were also observed at the P2 promoter, albeit to a lesser extent (Figure 1B and C). These results indicate that the silencer is involved in the initial deposition of H3K27me3 marks as well as in preventing premature H3K4me3 loading prior to positive selection.

Another known epigenetic modification involved in gene silencing is DNA methylation (Jones, 2012). We therefore next compared the DNA methylation status of the *Thpok* gene in $CD4^+$ and $CD8^+$ peripheral T cells. We tested 21 CpG islands derived from the *Thpok* silencer, distal P1 promoter, proximal P2 promoter and proximal enhancer (PE) and only three regions (S-4, 1-4 and 1-5) exhibited slightly increased DNA methylation in $CD8^+$ T cells compared to $CD4^+$ T cells (Figure 2A). Thus, our analyses did not detect any clear differences in the DNA methylation status of active versus repressed *Thpok* genes, although they could not formally exclude involvement of DNA methylation at other sites in repression of the *Thpok* gene.

To further examine roles of epigenetic modifications in *Thpok* repression, we treated $CD8^+$ T cells with Trichostatin A (TSA) or 5-aza-2′-deoxycytidine (5-AzaC), inhibitors of histone deacetylases (HDAC) and DNA methyltransferase, respectively. Three days after TSA treatment, *Thpok* expression in activated $CD8^+$ T cells was significantly increased specifically from the P1 promoter, albeit at a level still well below that in $CD4^+$ T cells. On the other hand, 5-AzaC induced a slight derepression of the *Thpok* gene mainly

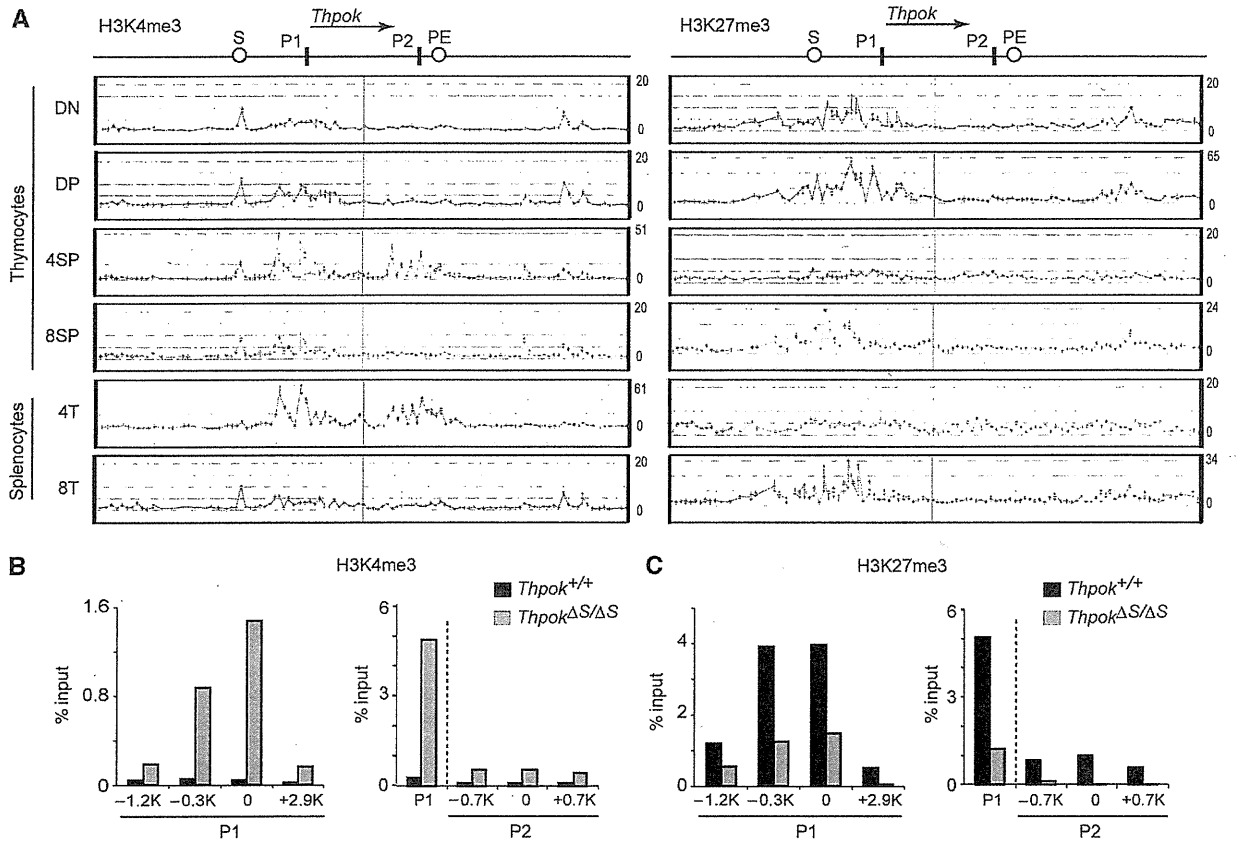

Figure 1 Changes of histone H3 modifications pattern in the *Thpok* gene during T-cell development. (**A**) Association of histone H3 K4 tri-methylation (H3K4me3) and histone H3 K27 tri-methylation (H3K27me3) in the *Thpok* locus. The signal intensities of individual oligonucleotide probe as revealed in a ChIP-on-chip assay in the indicated T-cell subsets are shown along with a schematic structure of the *Thpok* gene (top). Positions of the silencer (S), proximal enhancer (PE), distal P1 promoter (P1) and proximal P2 promoter (P2) are indicated. One representative result of two experiments is shown. (**B, C**) Comparison of H3K4me3 (**B**) and H3K27me3 (**C**) patterns at the region around the distal P1 and proximal P2 promoters between silencer-sufficient ($Thpok^{+/+}$) and -deficient ($Thpok^{\Delta S/\Delta S}$) DP thymocytes determined by analytical ChIP assays. Positions of each region analysed are shown as distance from the transcriptional start site in the P1 or P2 promoter-derived *Thpok* mRNA. In the panel shown at the right, the P1 promoter is also included as a reference. Data are from one of two independent experiments.

from the P2 promoter in a variegated manner (Figure 2B and C). Although it was not clear whether these inhibitors induced *Thpok* de-repression directly or indirectly, these results, along with the distinct H3K27me3 deposition pattern, suggested that different mechanisms are likely to be involved in preventing the activity of the two promoters for stable repression of the *Thpok* gene in $CD8^+$ T cells.

Conditional deletion of the Thpok silencer from CD8-lineage cells

Our result showed that lineage-specific chromatin structures are established at the *Thpok* locus and that this correlates with the presence of the *Thpok* silencer. To further investigate the relevance of such epigenetic modifications for the regulation of *Thpok* expression, we wished to test whether the repressive state is maintained independently of the silencer in differentiated $CD8^+$ T cells, as was observed at the *Cd4* locus (Zou *et al*, 2001). To this end, we have generated a $Thpok^{Sfl}$ allele in which an 800-bp region including the entire *Thpok* silencer sequence was flanked by two loxP sites (Supplementary Figure 1). The excision of the silencer in precursor DP thymocytes by *Cd4-Cre* transgene resulted in the loss of peripheral $CD8^+$ T cells, as was previously observed in the case of germline deletion of the silencer (Figure 3A; Setoguchi *et al*, 2008). On the contrary, deletion of the *Thpok* silencer in developing $CD4^-CD8^+$ SP thymocytes by *E8I-Cre* transgene (Maekawa *et al*, 2008), which is expressed after the cells have downregulated the CD24 surface marker, did not impair development of $CD8^+$ T cells (Figure 3A). Genotype analyses by Southern blot confirmed that the excision of the silencer by *E8I-Cre* was not at a detectable level in total thymocytes, but was almost complete in and restricted to $CD8^+$ cells among splenic T cells (Figure 3B). The level of *Thpok* mRNA in these silencer-deficient $CD8^+$ T cells was slightly elevated, but still <20% of that in $CD4^+$ T cells (Figure 3C). Thus, the conditional removal of the *Thpok* silencer from post-selection thymocytes differentiating into the cytotoxic lineage did not cause a massive de-repression of the *Thpok* gene. Interestingly, only P1-derived *Thpok* transcripts were detected in the $CD8^+$ T cells from $Thpok^{Sfl/Sfl}$;*E8I* mice (Figure 3D), whereas germline deletion of the silencer from a $Thpok^{gfp}$ reporter allele led to de-repression of the *gfp* gene from both the P1 and P2 promoters in $CD8^+$ T cells (Figure 3E).

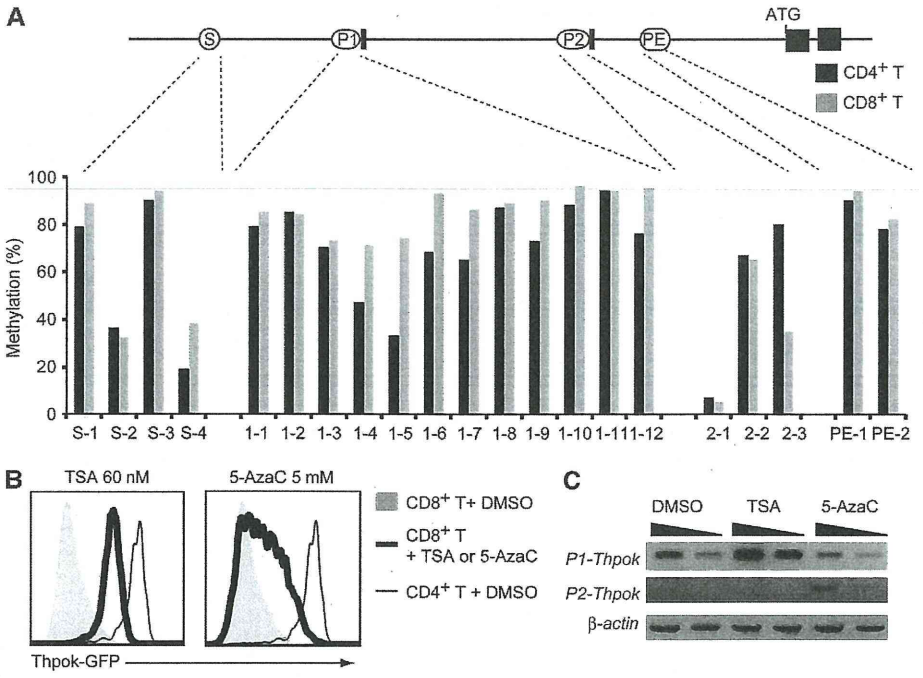

Figure 2 Comparison of DNA methylation status of the *Thpok* locus in CD4$^+$ and CD8$^+$ T cells. (**A**) DNA methylation status in CD4$^+$ and CD8$^+$ T cells analysed by methylation-specific PCR at selected CpG islands located within the silencer (S), distal P1 promoter (P1), proximal P2 promoter (P2) and proximal enhancer (PE) are shown as percentages. (**B**) Effects of chemical inhibitors of histone deacetylases, Trichostatin A (TSA), and DNA methyltransferase, 5-aza-2′-cytidine (5-AzaC), on the *Thpok* repression. Histograms showing Thpok-GFP expression from the *Thpok*^{gfp} allele in activated CD8$^+$ T cells 3 days after treatment with either inhibitor in culture. Expression of GFP in control CD4$^+$ T cells is shown as a thin line for reference. (**C**) Semi-quantitative RT–PCR for the P1 promoter- and the P2 promoter-derived *Thpok* mRNA after inhibitor treatment is shown with the β-*actin* mRNA as control. Wedges indicate 1:3 dilution of template. Data are from one of two independent experiments. Source data for this figure is available on the online supplementary information page.

We next examined the effect of deleting the *Thpok* silencer from fully differentiated CD8$^+$ T cells prepared from spleen. As previously reported (Setoguchi *et al*, 2009), Thpok-GFP expression was detected in activated CD8$^+$ T cells from the *Thpok*^{gfp} allele, but not the *Thpok*$^{gfp:\Delta PE}$ allele lacking the PE, after *in vitro* TCR stimulation (Figure 3F), indicating that the PE is necessary for *Thpok* expression in activated CD8$^+$ T cells. Both P1 and P2 promoter-derived *Thpok* mRNA was detected in activated CD4$^+$ T cells, however, activated CD8$^+$ T cells contained only the P1-derived *Thpok* mRNA (Figure 3G). When these CD4$^+$ and CD8$^+$ T cells from *Thpok*$^{Sfl/Sfl}$ mice were transduced with retroviral vectors encoding Cre recombinase, the silencer region was efficiently excised within 48 h (Figure 3H). However, the amount of *Thpok* mRNA in activated CD8$^+$ T cells was not elevated after removal of the silencer (Figure 3I) and the P2 promoter-derived *Thpok* mRNA remained undetectable (Figure 3J). These results demonstrate that sequential epigenetic modifications at the *Thpok* locus during commitment to the CD8$^+$ cytotoxic lineage in the thymus established an epigenetically repressed state that is maintained in peripheral CD8$^+$ T cells independently of the silencer.

Effect of enhanced Thpok silencer activity by increasing its copy number

It is known that increasing the copy number of a *cis*-regulatory region can enhance its function (Herr and Gluzman, 1985). Indeed, three copies of the *Thpok* silencer in a reporter plasmid repressed *luciferase* reporter expression more efficiently than one copy in a transfection assay (Supplementary Figure 2). We then wished to examine whether and how an increase in silencer copy number at the endogenous *Thpok* gene would affect its expression. To this end, we have generated a *Thpok*$^{gfp:3S}$ allele, in which three tandem copies of 202–401 core silencer sequences were inserted into the *Thpok*^{gfp} reporter allele by sequential gene targeting into ES cells of the *Thpok*$^{+/gfp}$ genotype (Supplementary Figure 3). Expression of GFP from the *Thpok*$^{gfp:3S}$ allele was analysed in *Thpok*$^{+/gfp:3S}$ mice, in which normal CD4$^+$ T-cell development is supported by the half dosage of ThPOK produced from the wild-type allele. The induction of GFP in the CD69$^+$ TCRβ^{hi} thymocyte subset from the *Thpok*$^{gfp:3S}$ allele was lower than from the control *Thpok*^{gfp} allele with respect to both expression levels and the percentage of GFP$^+$ cells (Figure 4A). Interestingly, GFP expression was lost in some CD4$^+$ T cells but was only reduced in other CD4$^+$ cells, thus exhibiting variegated repression rather than the uniform repression that was observed with the *Thpok*$^{gfp:\Delta PE}$ allele (Figure 4A). Since reduced GFP expression was not observed in non-T cells (Figure 4A), the effect of increasing silencer copy number was likely to be CD4-lineage specific rather than a general phenomenon in any types of cells.

To examine how impaired ThPOK expression due to the insertion of three copies of the *Thpok* silencer affects T-cell development, we have generated a *Thpok*^{3S} allele by targeting the same 3S mutation into the *Thpok* allele (Supplementary Figure 3). In *Thpok*$^{3S/3S}$ mice, the percentages of CD4$^+$CD8$^-$

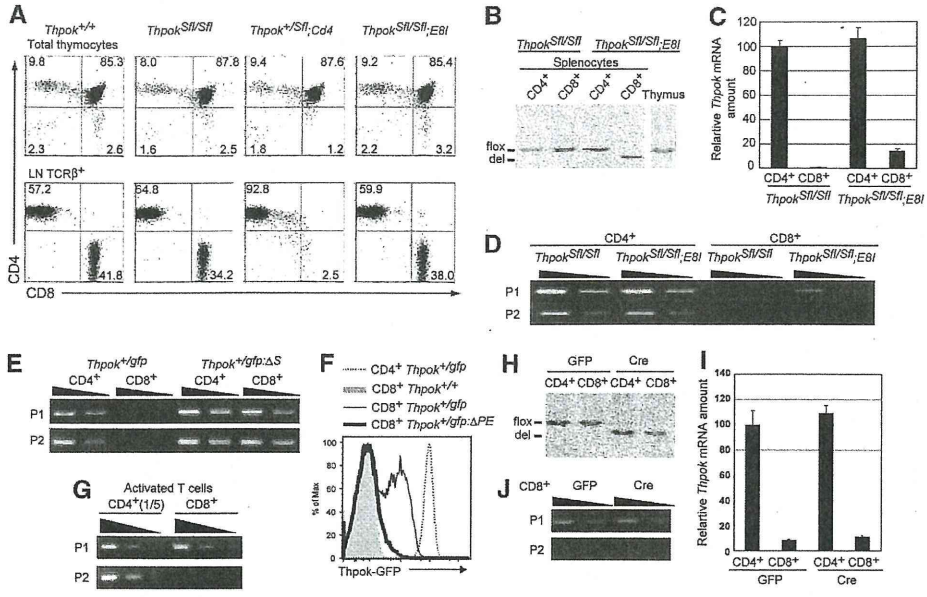

Figure 3 Effects of conditional removal of the *Thpok* silencer in CD8-lineage cells on *Thpok* expression. (**A**) Dot plots showing CD4 and CD8 expression in total thymocytes and lymph node TCRβ$^+$ T cells from mice of the indicated genotypes. Numbers in dot plots indicate the percentage of cells in each quadrant. (**B–D**) Genotype analyses by Southern blot (**B**), relative *Thpok* mRNA amounts (**C**) and semi-quantitative RT-PCR for the P1 promoter- and the P2 promoter-derived *Thpok* mRNA (**D**) in CD4$^+$ and CD8$^+$ T cells from the indicated mice. (**E, G**) Semi-quantitative RT–PCR for the P1 promoter- and the P2 promoter-derived *gfp* mRNA from the $Thpok^{gfp}$ and the silencer-deficient $Thpok^{gfp:\Delta S}$ allele in CD4$^+$ and CD8$^+$ T cells (**E**), and for the P1- and P2-derived *Thpok* mRNA in activated CD4$^+$ and CD8$^+$ T cells (**G**). (**F**) Histogram showing Thpok-GFP expression in the indicated activated T cells of indicated genotypes. (**H–J**) Genotype analyses by Southern blot (**H**), relative *Thpok* mRNA amount (**I**) and semi-quantitative RT–PCR for the P1 promoter- and the P2 promoter-derived *Thpok* mRNA (**J**) in activated CD4$^+$ and CD8$^+$ T cells from $Thpok^{Sfl/sfl}$ mice transduced with control retroviral vector (GFP) or vector encoding Cre recombinase (Cre). Wedges in semi-quantitative RT–PCR assay indicate 1:3 dilution of template, except in (**G**) (1:5 dilutions). Data are from one of at least two independent experiments. Source data for this figure is available on the online supplementary information page.

cells were reduced both in the thymus and in peripheral T-cell pools (Figure 4B). In $Thpok^{3S/gfp}$ mice in which ThPOK protein was produced only from the $ThPOK^{3S}$ allele, the decrease in the CD4$^+$ T-cell subset became more evident with emergence of CD8$^+$ T cells expressing GFP. Given that GFP expression from the $Thpok^{gfp}$ allele is specific to MHC class II-selected cells (Muroi *et al*, 2008), these CD8$^+$ GFP$^+$ cells are likely to be re-directed MHC class II-selected cells. Indeed, when we examined the differentiation of MHC class II-selected cells in mice with no surface expression of MHC class I molecules, cells with CD4$^-$CD8$^-$, CD4$^+$CD8$^+$ and CD4$^-$CD8$^+$ phenotype emerged in the peripheral lymphoid organs of $Thpok^{3S/3S}$ and $Thpok^{3S/gfp}$ mice whereas those cells were absent in control mice (Figure 4C). These observations indicated that enhanced *Thpok* silencer activity resulting from an increase in its copy number in the *Thpok* gene perturbed development of CD4$^+$ T cells via inhibiting *Thpok* expression in a variegated manner.

Possible epigenetic Thpok silencing in CD4-lineage cells

Variegated gene expression has been shown to be a characteristic of gene silencing mediated by heterochromatin-like structures (Weiler and Wakimoto, 1995). Given the variegated GFP expression from the $Thpok^{gfp:3S}$ allele in CD4$^+$ T cells and the epigenetic control of the *Thpok* locus that results in a silencer-independent maintenance of *Thpok* silencing in CD8-lineage cells, we next addressed whether an epigenetic repressive state, which is maintained independently of the silencers, is similarly established at the $Thpok^{gfp:3S}$ allele in CD4$^+$ helper-lineage cells. To this end, we have generated a $Thpok^{gfp:3SFRT}$ allele in which the three copies of the silencer can be excised upon expression of Flp recombinase (Figure 5A; Supplementary Figure 3). GFP expression from the $Thpok^{+/gfp:3SFRT}$ allele after *in vitro* TCR stimulation was still low in CD4$^+$ T cells and was not detected in activated CD8$^+$ T cells (Figure 5B). In addition, both P1 and P2 promoter-derived *gfp* mRNA was reduced in resting CD4$^+$ T cells from $Thpok^{+/gfp:3SFRT}$ mice (Figure 5C). Consistent with these observations, ChIP assays demonstrated an increase and decrease in H3K27me3 and H3K4me3 marks, respectively, at the region nearby the silencer on the $Thpok^{gfp:3SFRT}$ allele, compared to those on the wild-type *Thpok* allele in the same CD4$^+$ T cells of $Thpok^{+/gfp:3SFRT}$ mice (Figure 5D). Thus, chromatin structures at the $Thpok^{gfp:3SFRT}$ allele in CD4$^+$ T cells were similar to those at the wild-type *Thpok* allele in CD8$^+$ T cells. To examine whether GFP expression is restored if the three copies of the silencer are removed, we transduced CD4$^+$ T cells with a retroviral vector encoding Flp recombinase to obtain a population of cells in which the FRT-flanked silencers were efficiently excised (Figure 5E). Interestingly, the mean fluorescent intensity of GFP and *gfp* mRNA levels were not elevated after excision of the 3× silencer (Figure 5F and G), confirming that the silent state at the $Thpok^{gfp:3SFRT}$ allele in CD4$^+$ helper-lineage cells could be maintained in the absence of the three *Thpok* silencer copies. These genetic results clearly demonstrate that epigenetic *Thpok* silencing could be established not only in cytotoxic-lineage cells but